Geochemistry, Geophysics, Geosystems

Supporting Information for

Geometry of the deep Calabrian subduction (Central Mediterranean Sea) from wide-angle seismic data and 3-D gravity modeling.

David Dellong[1,4], Frauke Klingelhoefer[1], Anke Dannowski[2], Heidrun Kopp[2,3,] Shane Murphy[1], David Graindorge[4], Lucia Margheriti[5], Milena Moretti[5], Giovanni Barreca[6], Luciano Scarfi[7], Alina Polonia[8], Marc-Andre Gutscher[4]

(1) Géosciences Marines, IFREMER, Centre de Brest, Plouzané, France, (2) GEOMAR, Kiel, Germany, (3) Christian Albrechts University, Kiel, Germany (4) UMR LGO, University of Western Brittany, Brest, France (5) Istituto Nazionale di Geofisica e Vulcanologia (INGV)- Centro Nazionale Terremoti, Rome, Italy (6) Dipartimento di Scienze Biologiche, Geologiche ed Ambientali, University of Catania, Catania, Italy (7) Istituto Nazionale di Geofisica e Vulcanologia (INGV)- Osservatorio Etneo, Catania, Italy (8) ISMAR CNR, Bologna, Italy

Contents of this file

Introduction

This supporting information file shows wide-angle seismic data in a larger extend than the main manuscript (Text S1 and Figures S1-S3). It also shows additional detailed results from error calculations regarding the wide-angle seismic model (Text S2 and Figures S4-S5). Additional sections from the 3D model and a seperate higher resolution 2D gravity model are presented in Text S3 and Figures S6 – S8. Lastly Figure S9 is a 3D view of a zoom of the velocity models showing the position of the slab in detail

Text S1. 3-D gravity modeling methodology

The aim of the 3-D gravity modeling presented here was to reproduce the regional gravity anomaly closely using a simple geometry of layers while avoiding introducing small structures unconstrained by the relatively sparse

velocity models. Modeling was performed using the IGMAS+ software (Schmidt et al., 2010). The layers were constructed along fourteen 2-D parallel cross-sections the software interpolated in between these sections. Physical parameters were attributed to each layer. Subsequently, the gravity anomaly that these bodies produce was calculated on a grid of 10 km cell size. The modeled gravity anomaly was then compared to the free-air anomaly from the World Gravity Map (WGM-2012 – Bonvalot et al., 2012; Pavlis et al., 2012). As the area of investigation contains both land and offshore regions the complete Bouguer anomaly was not used, because the slab is expected to be deeper than the compensation depth of 30 km used to produce the WGM-2012 (Bonvalot et al., 2012).

Outside the area of interest that was constrained by the velocity models (densities and geometry), the 3D gravity models are extrapolated to fit the free-air anomaly data and to avoid side effects. The structures that are geographically distant from the wide-angle velocity models, were modeled using various sets of data such as MCS data for the shallow sedimentary structures (Casalbore et al., 2017; Minelli and Faccena, 2010; Gallais et al., 2012; Polonia et al., 2011; 2016); or tomographic models for the deeper crustal and mantelic structures (Spakman & Wortel, 2004; Wortel et al., 2009; Scarfi et al., 2018). Three different densities were used for the mantle layer based on the velocities of the tomographic models (Scarfi et al., 2018).. Regional earthquake hypocenters (INGV-ISIDe) and tomographic models were used to locate deep structures, especially the slab depth toward the N of the area of interest.

As the only sub-parallel profiles of the seismic experiment are DY-01 and DY-03, we used these in the first place to construct these models. The velocities of each layer were then converted into density using empirical relationships (Ludwig, Nafe & Drake 1979; Brocher, 2005). The calculations were done for a zero-level that was set at 3000 m (above sea-level) to avoid landmass effects,

To evaluate the impact of different configurations for the slab depth along the DYP3 profile, three different density models were constructed, were only the depth of the oceanic layer was modified to build the three density models. The first model is our (1) *reference model*, that was built to closely fit the predicted free-air anomaly from the model to the measured one. Then, two end-members models were built to test a (2) *shallow slab* hypothesis (5 km shallower slab) and a (3) *deep slab* hypothesis (15 km deeper).

The uncertainties were determined by identifying the smallest modification that significantly affects the resulting anomaly. The resulting uncertainties are of +/- 2.5 km for the top of the oceanic crust and the Moho interface.

Above these interfaces the uncertainties are smaller. The uncertainties are relatively high but do not negate the pertinence of the 3-D gravity models, as their main purpose was to explore the presence (or the absence) of a high density mantle layer between the Calabro-Peloritan backstops and the dipping oceanic slab along the DY-P3 velocity model and not to reproduce in fine detail the gravity anomaly.

Text S2. Additional error estimations

The model parametrization is important to make certain that the data are not overinterpreted and feature sizes modeled are adapted to the data quality (Figure S2 A). If the model is poorly resolved for a given region, then one given nodes's perturbation will be smeared into adjacent nodes, possibly for both the velocities and the boundary depths, if both parameter types are involved. Thus the extent of the smearing indicates the spatial resolution of the model (Zelt, 1999). Perturbing single nodes allows defining the spread-point function (SPF) giving the amount of smearing in different model regions (Figure S2 b).

The ray hit count is a measure of the number of rays passing through a particular area. It provides a measure of how well a section of the subsurface is resolved by the seismic survey (Figure S2 C). Although regions of low ray hit-count values are less well constrained, care was taken during modeling to use the minimum structure approach (Zelt, 1999) to avoid over-interpretation. Hit count values are high (> 5000) in the sedimentary layer and lower in the crustal layers. The least well covered domains are the Calabrian block and the upper mantle (< 2500).

Resolution is a measure of the number of rays passing one single of the user-defined velocity node and therefore depends on the number of nodes per layer. Nodes with a resolution larger than 0.5 are considered to be well resolved (Figure S2 D). Resolution is between 0.5 and 1.0 in the sedimentary layers except for the low velocity layer underneath the salt, where no turning rays are produced. A layer in which all rays pass by one single velocity node thus has a resolution of 1. The oceanic crustal layer and the upper crust of the Calabrian block are well resolved. However, the Calabrian lower crust and upper mantle yield lower values. The smearing factor gives information about the influence of perturbations of one single node onto the neighboring velocity and depth nodes (Zelt, 1999).

The "Vmontecarlo" software was used to produce a detailed analysis of the velocity uncertainties (Loureiro et al., 2016). 20000 independent random models were created, of which those who fit the threshold parameters in terms of number of picks modeled and rms travel-time residual were selected for an uncertainty analysis. The resulting uncertainty sections show a relatively good fit, with uncertainties not exceeding 1.0 km/s in the crustal layers (Figure S2).

Text S3. 2-D gravity modeling

Gravity is routinely used to confirm the structures imaged along wide-angle seismic models. As it is not possible to extract a section corresponding exactly to the DY-04 model using the IGMAS+ software, additional modelling was undertaken using the “xgravmod” of Colin Zelt (Zelt, 1999; Figure 13). This model takes into account the densities from the seismic velocities modeled in the sedimentary and oceanic crustal sections and the mantle velocities from the 3D gravity modeling for all other regions. A linear trend corresponding to large scale variations and the influence of the slab at depth larger than our model was subtracted. The good fit of this 2D model confirms the validity of both the 3D gravity and the velocity model.

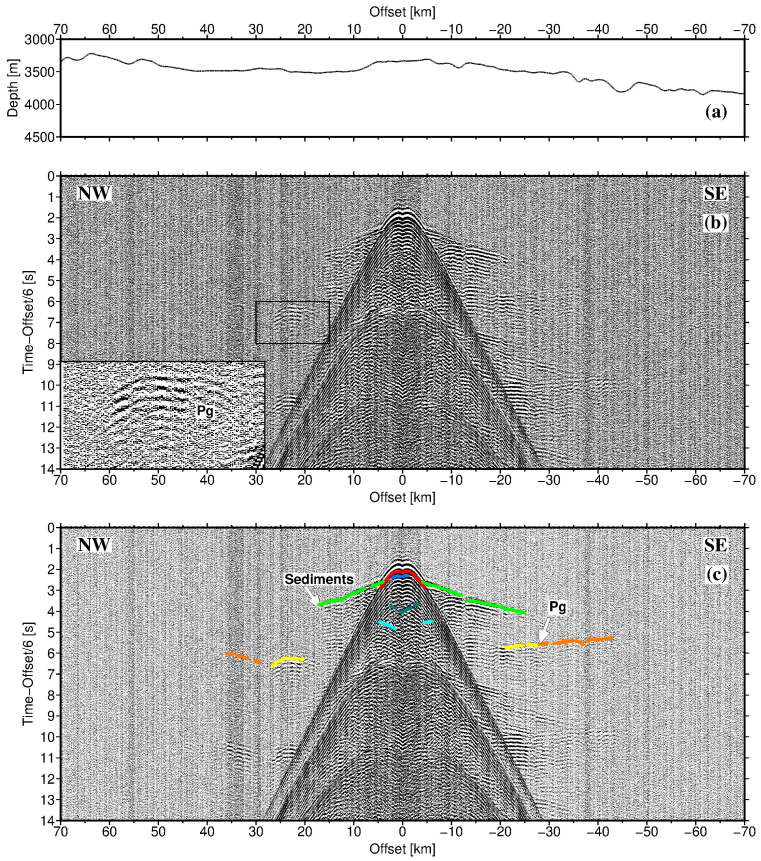

Figure S1. Seafloor bathymetry along the sections shown below (b) Data section from OBS 20 vertical geophone channel. The data are bandpass filtered (3-4-24-36 Hz corner frequencies) and reduced to a velocity of 6 km/s (c) Data section OBS 20 with travel-time picks overlain.

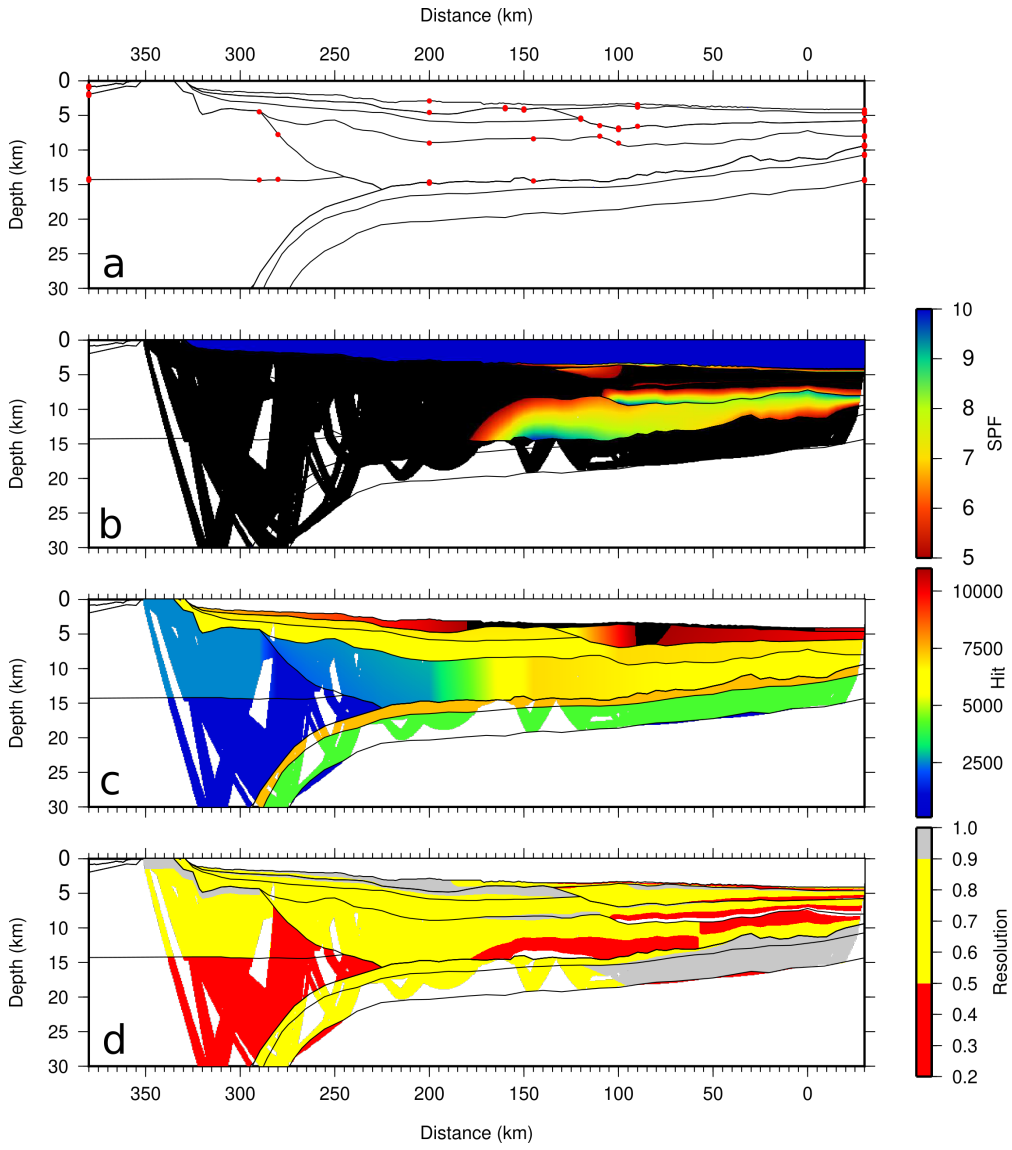

Figure S2. Error estimation of the velocity model (a) Model parameterization including interface depth, top and bottom layer velocity nodes (red circles) (b) Spread-Point function (SPF) for velocity (gridded and coloured) nodes (c) Hit count for velocity (gridded and coloured) nodes (d) Resolution of velocity (gridded and coloured) and depth nodes (squares)

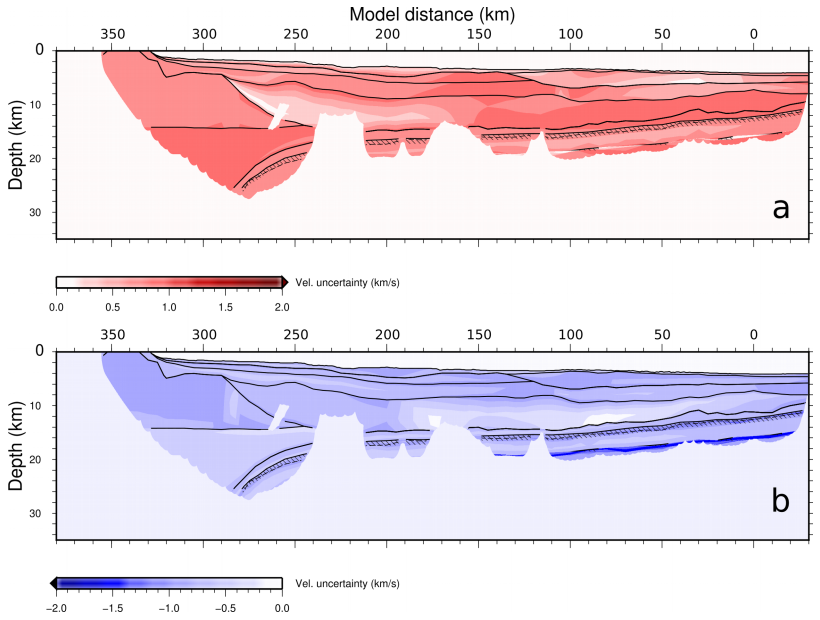

Figure S3. General uncertainty plot of profile DYP4 from Monte Carlo modeling. a) Maximum and b) minimum admissible velocity deviations from the preferred model, built from 145 models capable of tracing at least 22772 rays (95% of the preferred model), with an RMS value under 199 ms (150% of the preferred model).

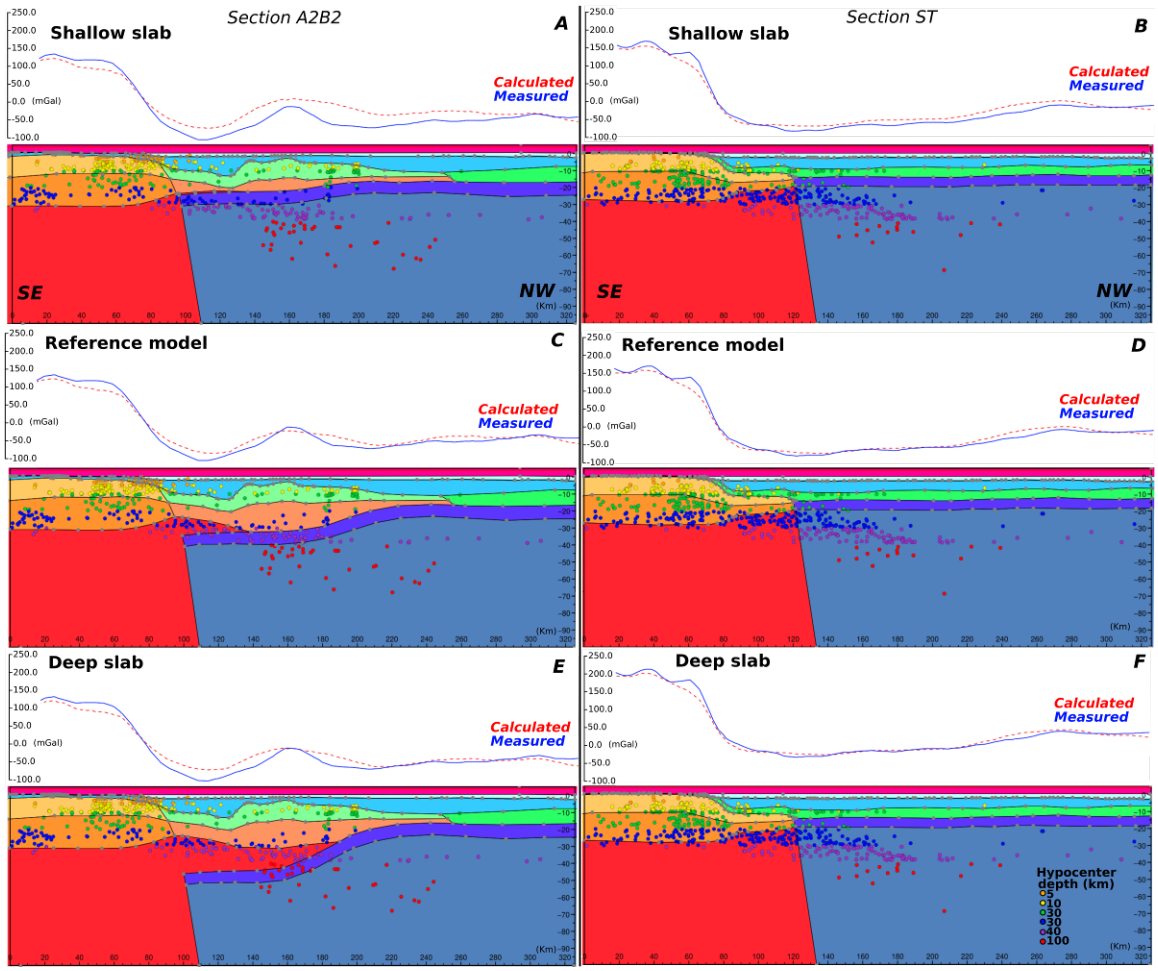

Figure S4. Two 2D gravity cross-sections extracted from the three 3-D gravity models (left: A2B2; right ST; location marked in Figure 1). The three scenarios are shown: shallow slab (A,B), the reference model (C,D) and the deep slab model (E,F). For each scenario, the upper panels show the calculated (red line) and measured (blue line) gravity anomaly, while the bottom panel shows the density models. Layers density, names and velocity are shown in Table 2 with corresponding colors. Earthquake hypocenters projected from 10 km onto the profile are shown by small circles colored by depth.

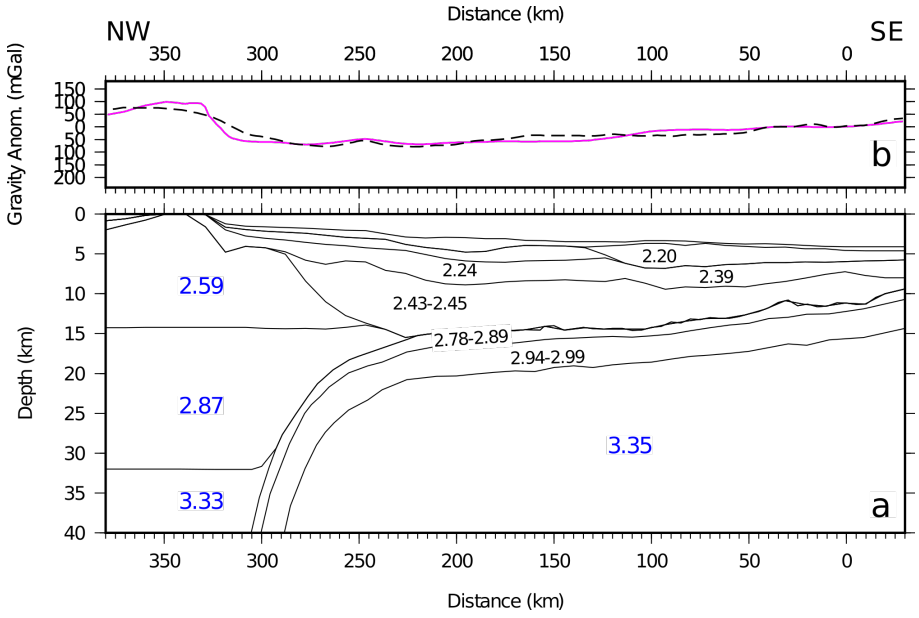

Figure S5. 2D gravity model corresponding to the seismic velocity model DY-04. Black numbers are densities calculated from the velocities of the velocity model and blue numbers densities from the 3D gravity model.

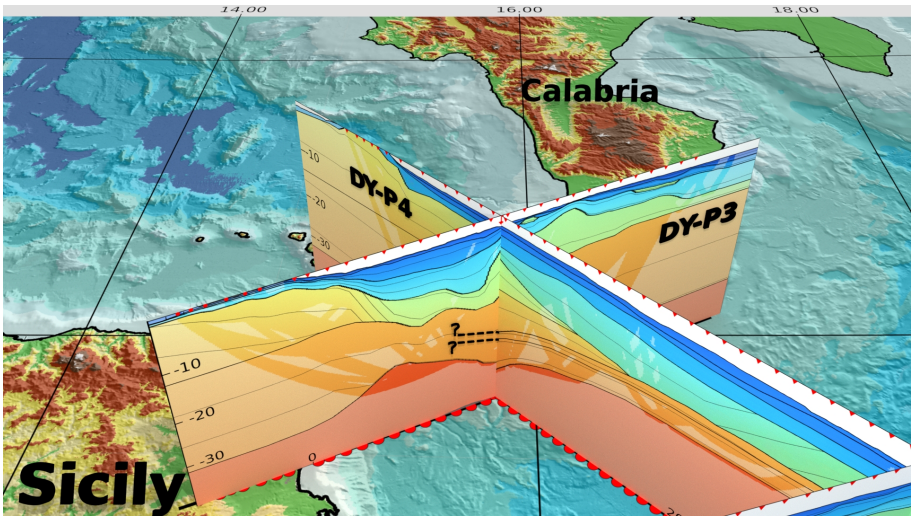

Figure S6. 3-D view of the velocity models DY-P4 crossing the DY-P3 above the bathymetric map (Figure 1 & 2). Dashed lines show the extension of the oceanic upper crustal layer (from DY-P4) onto the DY-P3 velocity model and good agreement of the Moho depth between both models.

Layer Name	Velocity ($km.s^{-1}$)	Density ($g.cm^{-3}$)
Water	1.5	1
Sediments	2.39	2.3
Fast seds	4.6	2.49
Upper-Crust Sicily	6.2	2.63
Lower-Crust Sicily	6.85	2.88
Upper-Crust Calabria	4.95	2.59
Lower-Crust Calabria	6.75	2.87
One layer Oceanic Crust	6.6	2.8
Mantle	8.1	3.33
Back-arc Mantle		3.22
Oceanic Mantle		3.35
Reference	8.1	3.33

Table S1. Layers and densities used for the gravity modelling. Densities are extracted from the velocity models DY-P3 and DY-P1 (Dellong et al., 2018, velocity mean of the layers). Velocities are then converted to densities using the empirical relationships between these parameters (Ludwig, Nafe & Drake 1979, Brocher, 2005).